Virtual Attractive-Repulsive Potentials for Cooperative Control of Second Order Dynamic Vehicles on the Caltech MVWT

Bao Q. Nguyen[1], Yao-Li Chuang[2], David Tung[3], Chung Hsieh[1],
Zhipu Jin[4], Ling Shi[5], Daniel Marthaler[6], Andrea Bertozzi[6], Richard M. Murray[5]

***Abstract*— We consider a motion planning method based on cooperative biological swarming models with virtual attractive and repulsive potentials (VARP). We derive a map between the model and fan speeds for the Kelly, a second order vehicle on the Caltech Multi Vehicle Wireless Testbed. The motion planning map results leads to the development and implementation of a point to point controller which is subsequently used as part of a cooperative searching algorithm. The VARP control method is scalable and can be used to organize a swarm of robotic vehicles.**

I. Introduction

Virtual potentials provide a convenient framework for autonomous vehicle control and path planning. Recent control applications include coordinated group motion with artificial leaders [9], obstacle avoidance [11], and maintaining an automobile's lane position on a highway [14]. There are several mathematical frameworks proposed for the construction of the artificial potential field. They include harmonic functions and Laplace's equation [1, 2] stream functions from fluid dynamics [16] and pairwise virtual attractive-repulsive potentials (VARP) for point masses. We are interested in the last type of potentials for two reasons. First, their representation as virtual force laws make them straightforward to port on second order vehicles propelled by mechanisms that directly impart a force to the vehicle. Secondly, such pairwise interactions can yield complex group behavior using very simple, scalable algorithms, thus making these methods very interesting for cooperative motion problems involving many vehicles. Such virtual potentials arise in swarming models in biology [4, 6, 10, 12] and lead to interesting patterns including milling and flocking for collective motion. The testbed implementation here is a first step towards bringing ideas from these biological applications to coordinate motion of large groups of vehicles.

In this paper we demonstrate experimentally, with second order control vehicles, that it is very straightforward to map virtual potential laws directly to onboard vehicle propulsive functions and that such control algorithms can be used for motion planning. This approach is quite scalable and thus could be used for platforms of many robots. Our experiments are carried out on the Caltech Multi Vehicle Wireless Testbed [5] which offers a group of vehicles, named "Kelly", driven by ducted fans. We describe our method for mapping the virtual potential cooperative motion equations directly to fan controls for the Kellys. The VARP method allows us to define an open loop point to point controller for the Kelly by placing a virtual potential at the new target point for the vehicle. We show experimental results of cooperative searching with two Kellys using the VARP controller.

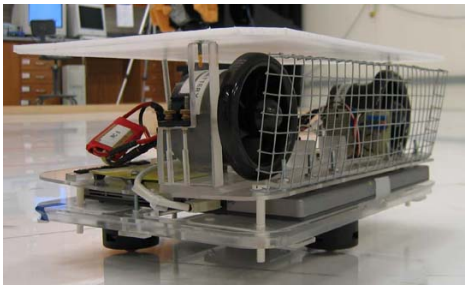

Fig. 1. The vehicle Kelly at the Caltech MVWT.

II. The Caltech MVWT

The Caltech Multi-Vehicle Wireless Testbed (MVWT) is a platform designed for experiments involving cooperative multi-vehicle control. The MVWT consists of vehicles with the ability to communicate over a wireless network, an arena for multi-vehicle operations, a Lab Positioning System using overhead cameras, and an offboard computer network. Each vehicle in the MVWT has an onboard computer, onboard sensors, and an 802.11b wireless Ethernet card. There is a smooth floor with dimensions of approximately 6.5 m x 7.0 m with a center pole. The vehicles are marked with binary symbols on their hats, which the vision system uses to identify each vehicle's position and orientation. Readers are referred to [5] for details of the Caltech MVWT.

Fig. 1 shows the Kelly with two ducted fans, which propel the vehicle. The controller governs the Kelly's motion through the fan force generating subroutines. For a pair of specific left and right fan forces, F_L and F_R, the Kelly's equations of motion [8] are:

[1]Dept. of Electrical Engineering, UCLA, Los Angeles, CA 90095 bknguyen@ucla.edu, chung_hsieh@ieee.org
[2]Dept. of Physics, Duke University, Durham, NC 27708 chuang@math.ucla.edu
[3]Dept. of Computer Science, UCLA, Los Angeles, CA 90095 davetung@ucla.edu
[4]Dept. of Electrical Engineering, California Institute of Technology, Pasadena, CA 91125 jzp@cds.caltech.edu
[5]Control and Dynamical Systems, California Institute of Technology, Pasadena, CA 91125 {shiling, murray}@cds.caltech.edu
[6]Dept. of Mathematics, UCLA, Los Angeles, CA 90095 {daniel, bertozzi}@math.ucla.edu

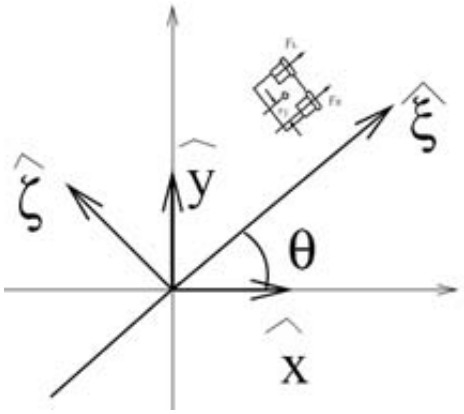

Fig. 2. Two Cartesian coordinate systems used to describe the position and velocity of the Kelly. The $x-y$ coordinates are fixed on the ground while the $\xi-\zeta$ coordinates are attached to the vehicle; ξ points to the direction of the vehicle's linear motion and ζ is perpendicular to ξ. The rotation angle between these two coordinate systems is denoted by θ.

$$m\frac{du}{dt} = -\mu u + (F_R + F_L)\cos\theta, \quad (1)$$

$$m\frac{dv}{dt} = -\mu v + (F_R + F_L)\sin\theta, \quad (2)$$

$$J\frac{d\Omega}{dt} = -\psi\Omega + (F_R - F_L)\, r_f. \quad (3)$$

In the above equations, F_R and F_L are the output forces of the right and left fans, which are separated by a distance of $2r_f$. The mass of the vehicle is m. The linear and angular friction coefficients are μ and ψ, respectively. The components of the linear velocity of the vehicle are $u = \frac{dx}{dt}$ and $v = \frac{dy}{dt}$, where x and y are the position coordinates of the vehicle, respectively. The angular velocity relative to the $x-y$ coordinates is $\Omega = \frac{d\theta}{dt}$, where θ is the orientation of the vehicle, as shown in Fig. 2. If the vehicle in Fig. 2 is labelled as the i-th vehicle, then we write θ as θ_i, $\hat{\xi}$ as $\hat{\xi}_i$, etc. The two coordinate systems describing the Kelly's motion are shown in Fig. 2.

Equation (1) and (2) are specified on the x-y frame, which is fixed on the testbed and does not depend on the orientation of the vehicle. On the other hand, the rotation equation (3) describes a force that is perpendicular to the direction of the vehicle's velocity. Therefore, it requires a second Cartesian system ξ-ζ that rotates with the vehicle. The unit vector $\hat{\xi}$ points in the direction of the vehicle's motion while the unit vector $\hat{\zeta}$ is perpendicular to it. Any second order model that is intended to directly access the fan force generator to drive the vehicle has to project its force law onto these two coordinate systems in order to link the model parameters to the controlling factors.

III. VARP Theory

Given N agents labelled $i = 1, ..., N$ at position $z_i = (x_i, y_i)$, consider the following general coupled equations of motion

$$\begin{aligned} \frac{d\vec{z}_i}{dt} &= \vec{w}_i, \\ m\frac{d\vec{w}_i}{dt} &= \alpha\hat{\xi}_i - \beta\vec{w}_i - \nabla_{\vec{z}_i}\sum_{j(j\neq i)}[-V_a(\|\triangle\vec{z}_{ij}\|) \\ &\quad + V_r(\|\triangle\vec{z}_{ij}\|)], \end{aligned} \quad (4)$$

where $\triangle\vec{z}_{ij} = \vec{z}_i - \vec{z}_j$; $\vec{z}_i$, $\vec{w}_i$ represent the position and velocity of the i-th agent; α is the magnitude of a self propulsion force; β is a friction coefficient; and $V_a(x)$, $V_r(x)$ are the attractive and repulsive potential functions. This model is proposed in [10] for collective motion in biology and has some things in common with recently proposed control methods involving virtual potentials [9, 11, 14, 16]. In [10] the potentials serve to organize a group of self-propelled particles into a mill-like formation. In the testbed examples presented here, we use equation (4) with attractive potentials as to direct vehicles towards way points and attractive/repulsive potentials to keep vehicles from avoiding each other and stationary obstacles. Thus the 'agents' labelled j in the above model will correspond to fixed way points or obstacles instead of other vehicles.

Leonard and Fiorelli [9] use similar artificial potentials to direct the motion of the vehicles. However, they use a fixed reference velocity with a dissipation model to control overall direction of flight. The virtual potentials in their model then serve to create and maintain group formation. In our model there is no fixed reference velocity. Without potentials, the vehicle's direction is uncontrolled and the vehicle's speed equilibrates to $\frac{\alpha}{\beta}$. Such motion can be subject to compounded noise and errors when acting alone, however, as we demonstrate below, with additional potentials the orientation of the vehicle is automatically corrected to head towards the point of interest. Also this allows us to use potentials to direct motion from a distance instead of using a reference velocity.

Our goal is to implement the swarming equation on the Kellys. Thus we need to find a map from equation (4) to the Kelly's motion (1-3), which allows us to determine the fan speeds based on the propulsion and drag parameters and locations of artificial potentials. In order to do this, we need to project equation (4) onto the coordinate system adopted by the Kelly's controller. Equation (1) and (2) are in x-y coordinates while equation (3) involves motion in an internal reference frame. Writing the force law in equation (4) as a combination of two components: one perpendicular to $\vec{w}_i$, which corresponds to equation (3); and the other is parallel to it, which is further separated into x and y components, corresponding to equation (1) and equation (2) respectively.

The x-parallel component is

$$\frac{mdu_i}{dt} = \alpha\cos\theta_i - \beta u_i + \sum_{j(j\neq i)}\{[V_a'(\|\triangle\vec{z}_{ij}\|) - V_r'(\|\triangle\vec{z}_{ij}\|)] \cdot\frac{(x_i-x_j)\cos^2\theta_i + (y_i-y_j)\cos\theta_i\sin\theta_i}{\|\triangle\vec{z}_{ij}\|}\}, \quad (5)$$

while the y-parallel component is

$$\frac{mdv_i}{dt} = \alpha\sin\theta_i - \beta v_i + \sum_{j(j\neq i)}\{[V_a'(\|\triangle\vec{z}_{ij}\|) - V_r'(\|\triangle\vec{z}_{ij}\|)] \cdot\frac{(x_i-x_j)\cos\theta_i\sin\theta_i + (y_i-y_j)\sin^2\theta_i}{\|\triangle\vec{z}_{ij}\|}\}, \quad (6)$$

where V_a' and V_r' represent the first derivatives of V_a and V_r, respectively. The remaining perpendicular component:

$$\left.\frac{md\vec{w}_i}{dt}\right|_{\perp} = \sum_{j(j\neq i)}\{[V_a'(\|\triangle\vec{z}_{ij}\|) - V_r'(\|\triangle\vec{z}_{ij}\|)] \cdot\frac{-(x_i-x_j)\sin\theta_i + (y_i-y_j)\cos\theta_i}{\|\triangle\vec{z}_{ij}\|}\hat{\xi}\},$$

can be re-written as the change of angular momentum:

$$J\frac{d\Omega_i}{dt} = r_f\sum_{j(j\neq i)}\{[V_a'(\|\triangle\vec{z}_{ij}\|) - V_r'(\|\triangle\vec{z}_{ij}\|)] \cdot\frac{-(x_i-x_j)\sin\theta_i + (y_i-y_j)\cos\theta_i}{\|\triangle\vec{z}_{ij}\|}\}. \quad (7)$$

Note that there is a length of r_f multiplied on the right hand side. This is because the turning radius is the half-width of the vehicle r_f by utilizing the spinning to change the direction of the vehicle's motion.

Comparing the Kelly's equations (1, 2, 3) and those of the swarming model (5, 6, 7) we can immediately relate their parameters.

$$\mu = \beta, \quad (8)$$

$$(F_R+F_L) = \alpha + \sum_{j(j\neq i)}\{[V_a'(\|\triangle\vec{z}_{ij}\|) - V_r'(\|\triangle\vec{z}_{ij}\|)] \cdot\frac{(x_i-x_j)\cos\theta_i + (y_i-y_j)\sin\theta_i}{\|\triangle\vec{z}_{ij}\|}\}, \quad (9)$$

$$\psi = 0, \quad (10)$$

$$(F_R-F_L) = -\sum_{j(j\neq i)}\{[V_a'(\|\triangle\vec{z}_{ij}\|) - V_r'(\|\triangle\vec{z}_{ij}\|)] \cdot\frac{(x_i-x_j)\sin\theta_i - (y_i-y_j)\cos\theta_i}{\|\triangle\vec{z}_{ij}\|}\}. \quad (11)$$

The equation (10) has no rotation and thus we ignore the rotational friction in equation (10). This discrepancy does not appear to adversely effect the performance on the testbed.

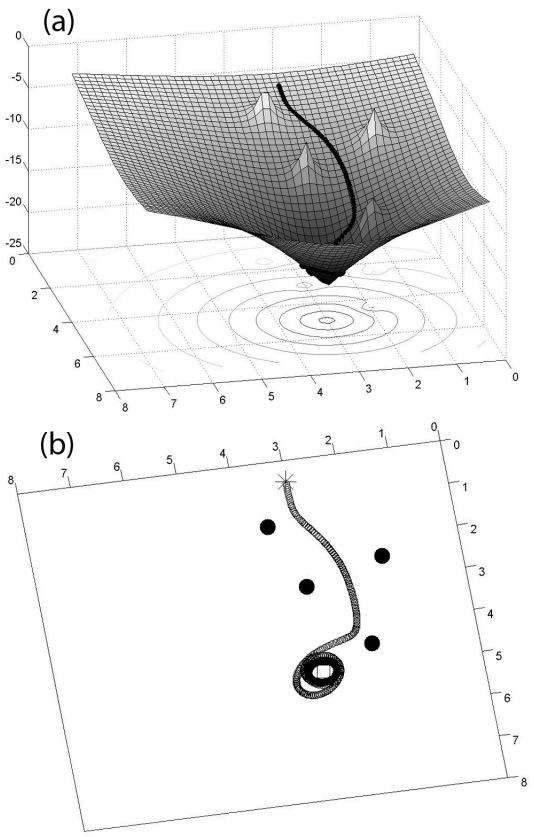

Fig. 3. Simulations. Mapping of virtual attractive and repulsive potentials for autonomous vehicular control and guidance. Parameters for: (i) the vehicle: α = 0.066 N, β = 5.05 Kgs^{-1}, (ii) the attractive point: C_a = 3 Nm, l_a = 3.5 m, C_r = 0 Nm; (iii) the repulsive points: C_a = 0 Nm, C_r = 5 Nm, l_r = 0.15 m. (a) Potential map: vehicle is driven from high potential to low potential, indicated by the darker curve, and the contour of the potential map in $\mathbb{R}^3$, the peaks are the repulsive potential points, the well is the attractive point. (b) The trajectory of vehicle in $\mathbb{R}^2$, solid black dots represent obstacles, starting point is indicated by *, the destination point is indicated by a square.

Finally, the specific VARP fan force controller is obtained by solving equation (9) and (11) for F_R and F_L; the results are:

$$F_R = \frac{\alpha}{2} + (\cos\theta_i - \sin\theta_i)F_{1,i} + (\sin\theta_i + \cos\theta_i)F_{2,i},$$
$$F_L = \frac{\alpha}{2} + (\cos\theta_i + \sin\theta_i)F_{1,i} + (\sin\theta_i - \cos\theta_i)F_{2,i},$$

where

$$F_{1,i} = \sum_{j(j\neq i)}\left\{[V_a'(\|\triangle\vec{z}_{ij}\|) - V_r'(\|\triangle\vec{z}_{ij}\|)]\frac{(x_i-x_j)}{\|\triangle\vec{z}_{ij}\|}\right\},$$
$$F_{2,i} = \sum_{j(j\neq i)}\left\{[V_a'(\|\triangle\vec{z}_{ij}\|) - V_r'(\|\triangle\vec{z}_{ij}\|)]\frac{(y_i-y_j)}{\|\triangle\vec{z}_{ij}\|}\right\}.$$

IV. VARP Properties

The VARP controller has the following properties:

1) Self propulsion: controlled by α.

2) Virtual attractive potential: controlled by C_a and l_a.
3) Virtual repulsive potential: controlled by C_r and l_r.

An attractive potential point is the analog of a valley, where a vehicle prefers to go to. Similarly, a repulsive potential point is the analog of a mountain, which a vehicle avoids. The potential mountains can be used to guide the vehicle in a desired path while navigating to the target location. For example, Fig. 3 shows a simulation with four repulsive potentials and one large attractive potential at a target point. Making the attractive characteristic length long enough allows the vehicle to go to it while avoiding the repulsive points. Fig. 3(a) shows the vehicle on the potential map and Fig. 3(b) shows the vehicle on a plane.

In this paper we use the VARP control method to move vehicles from one point to another while avoiding obstacles. The velocity of the vehicle can be controlled by (a) specifying the depth of the valley, which is controlled by varying the attraction gain and attraction characteristic length and (b) changing the self propulsion force α. The repulsive characteristic length l_r must be less than the characteristic distance between the obstacles, otherwise a local well may form that traps the vehicle. The constant self propulsive force α in this simulation causes the vehicle to orbit the target point once it arrives there.

V. Experimental Results

To implement the idea of the VARP method on the testbed, specific potential functions are chosen in the experiment:

$$\begin{aligned} V_a(z) &= C_a e^{-z/l_a}, \\ V_r(z) &= C_r e^{-z/l_r}, \end{aligned}$$

where C_a and C_r represent the potential strength respectively while l_a and l_r are their characteritc lengths correspondingly.

A. Attractive Point

We place a virtual attractive potential at (5, 5) and place the vehicle approximately four meters from the target. We compare the dynamics for different initial orientation angles θ with respect to the vector from the initial vehicle location to the target site. Fig. 4 shows four cases with $\theta = 0°$, $45°$, $80°$, $166°$, respectively. The vehicle self propulsion force is $\alpha = 0.6$ N, the drag $\beta = 5.05\ Kgs^{-1}$, and the attractive potential parameters $C_a = 0.06$ Nm, $l_a = 4$ m, $C_r = 0$. In all four cases the vehicle automatically orients itself towards the target and reaches its goal.

It is interesting to note in Fig. 4(a), despite the starting angle of $0°$ the vehicle's path is not a straight line. This phenomenon is mainly caused by the offset between left fan and the right fan. We verify this in a simulation, Fig. 5, which shows: (a) the vehicle runs straight to the target site under ideal conditions; (b) the vehicle deviates from the ideal path under the fan force offset condition. Under both ideal and non ideal conditions, the vehicle reaches its target site. In practice, the fan offset varies among the vehicles and from time to time; the VARP control method shows its robustness against a reasonable magnitude of fan offset.

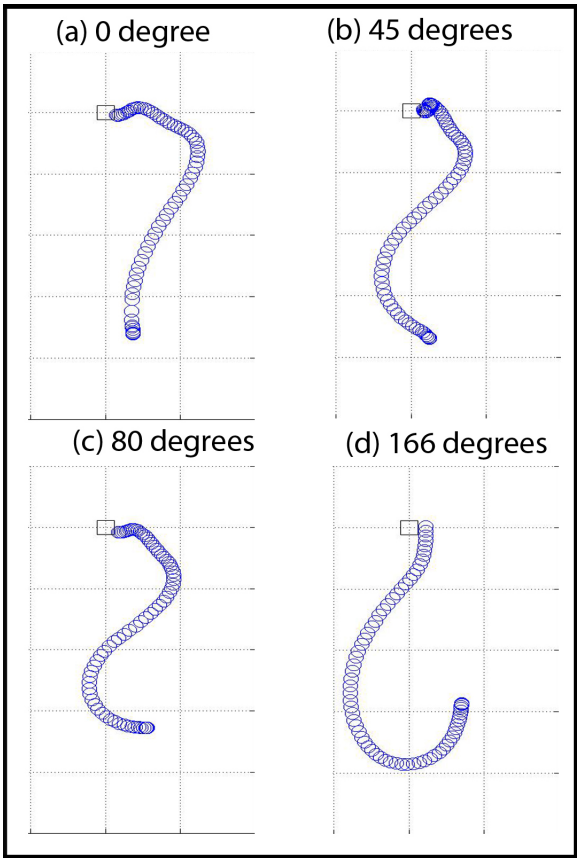

Fig. 4. Trajectory of Kelly running to the target location at (5, 5), indicated by a square, from arbitrary points, approximately 4 meters away, starting with different angles from facing the target point: (a) $0°$, runtime: t = 7.8 sec, (b) $45°$, runtime: t = 8.9 sec, (c) $80°$, runtime: t = 9.1 sec, (d) $166°$, runtime: t = 10.5 sec. Parameters for: (i) the vehicle: $\alpha = 0.6$ N, $\beta = 5.05$ Kgs^{-1}; (ii) the target: $C_a = 0.06$ Nm, $l_a = 4$ m, $C_r = 0$. Grid is 1x1 meter, o represents the Kelly's path, a square represents the target.

B. Avoiding stationary Obstacle

The Caltech MVWT has a central pole that must be avoided in path planning. We put a repulsive artificial potential at the pole location to keep vehicles from running into it. Variations in the repulsive strength and characteristic length correspond to changes in magnitude of repulsion and radius of repulsion, respectively. With just a repulsive force the vehicle motion is pushed too far off course. This is also noted in [16]. By using a combination of attractive and repulsive forces the vehicle avoids the post and returns to its planned trajectory as shown in Fig. 6. This is a simple alternative to the stream function method [16]. Fig. 6 shows the Kelly's trajectory, and Fig. 7 is the profile of the Kelly's fan forces.

C. Avoiding Multiple Obstacles

On the Caltech MVWT, four obstacles are placed between the Kelly and its target site. We set the attraction and

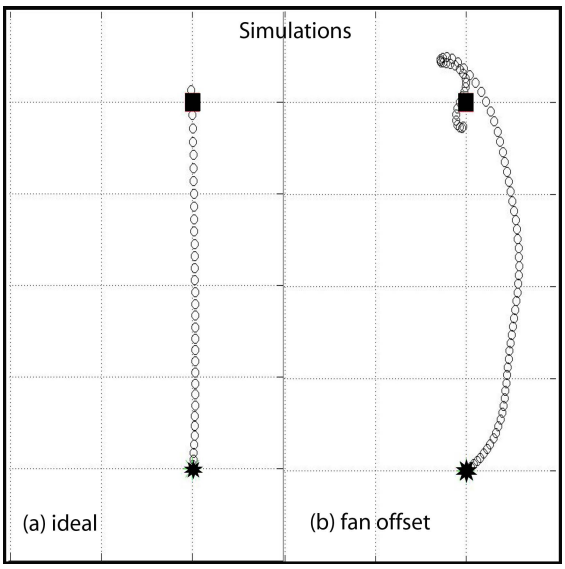

Fig. 5. Simulations. The trajectory of one agent running from (1, 1), indicated by *, with 0 degree from facing the target site at (5, 5), indicated by a square. Parameters for: (i) the vehicle: α = 1.0 N, β = 5.05 Kgs^{-1}; (ii) the attractive point: C_a = 1.0, l_a = 3, C_r = 0. (a) Ideal case: left fan and right fan are identical. (b) Offset modeled case: imitating the offset between left fan and right fan of the real vehicle by 0.6 N.

repulsion so that the potential space has no local minima to trap the Kelly. In Fig. 8 shows the Kelly's trajectory while avoiding the obstacles. This experimental result is similar to the matlab simulation in Fig. 3.

D. VARP Controller in Multi-Agent Searchers

The VARP controller is easily scalable to more than one vehicle. We use the VARP controller in the implementation of a greedy search algorithm [3, 15], in which the Kellys cooperatively search a list of spatial targets. In this algorithm, each Kelly selects the closest available target on the list and moves to that target. If two Kellys have selected the same target, the one that is further away will select another target. The Kellys also communicate the list of targets that they have already searched to prevent redundant searches. The VARP method moves the vehicles from point to point. The virtual attractive potential is placed at the selected target site and is removed once the vehicle reaches that point.

Fig. 9 shows the trajectories of two Kellys performing the greedy search algorithm with four targets and limited communication range of 1.5 m. The Kellys run toward the closest target and arbitrate their target selection when they are within communication range as shown in Fig. 9(a). The Kellys then move to their selected targets, shown in Fig. 9(b) and Fig. 9(c), until the last one is reached and their target lists are communicated, as shown in Fig. 9(d).

VI. Summary and Future Work

This paper presents a decentralized control method for nonlinear second order dynamic vehicles. We also show that the virtual attractive-repulsive potentials provide a

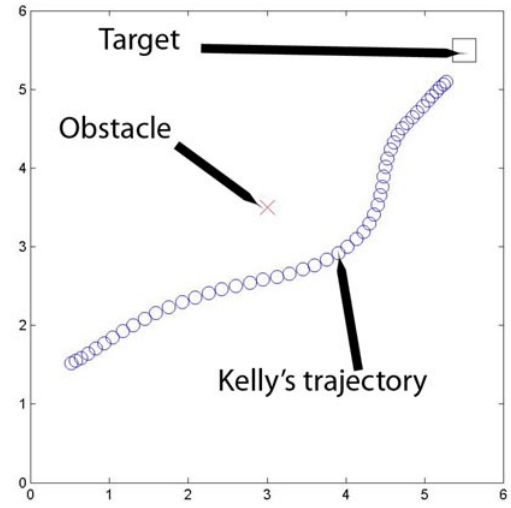

Fig. 6. Kelly avoids object while running to its target location. Parameters: (i) for the vehicle: $\alpha = 0.6$ N, $\beta = 5.05$ Kgs^{-1}; (ii) for the target point: s^{-1}, $C_a = 1.01$ Nm, $l_a = 4$ m, $C_r = 0$; (ii) for the obstacle: $C_a = 0.5$ Nm, $C_r = 1.0$ Nm , $l_a = 0.5$ m, $l_r = 0.3$ m.

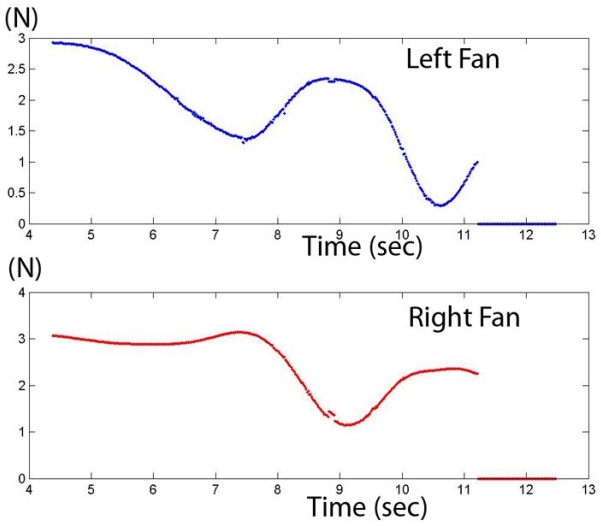

Fig. 7. Profile of the Kelly's fan forces in obstacle avoidance in Fig. 6.

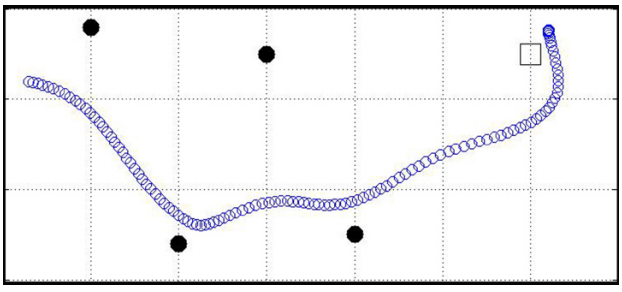

Fig. 8. Kelly navigates through the obstacles (solid black circles) to the target site (the square). Parameters for: (i) the vehicle: $\alpha = 0.6$ N, $\beta = 5.05$ Kgs^{-1}; (ii) the target: $C_a = 1.01$ Nm, $l_a = 4$ m; (iii) the obstacles: $C_a = 0.5$ Nm, $l_a = 0.5$ m, $C_r = 1.0$ Nm, $l_r = 0.3$ m. Grid is 1x1 meter.

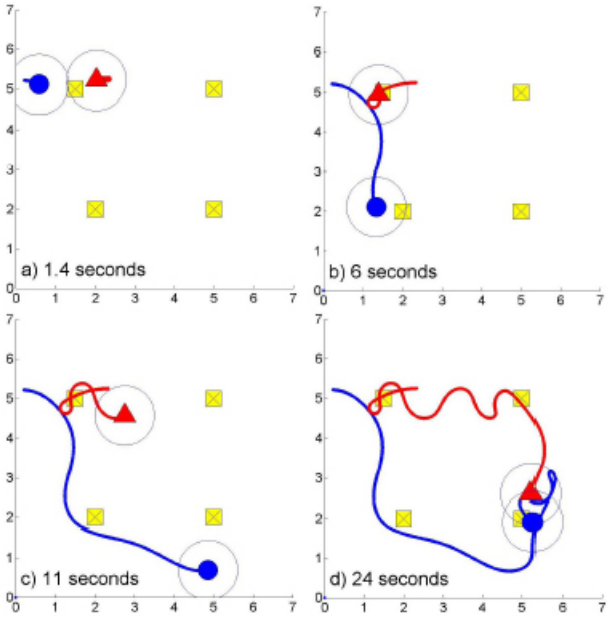

Fig. 9. Using the VARP controller: two Kellys performing the greedy search algorithm with the VARP controller. Four squares with the x marks represent four targets. The circle and triangle represent the vehicles' current locations. The solid lines that follow them are their paths. The communication range is 1.5 m, so the circles around the vehicles have radii of 0.75 m. Grid is 1x1 meter. Parameters: (i) for the vehicle: $\alpha = 2.6$ N, $\beta = 5.05$ Kgs^{-1}; (ii) for the attractive point: $C_a = 1.01$ Nm, $l_a = 4$ m, $C_r = 0$ Nm; (iii) for the moving obstacle (other Kelly): $C_a = 0$ Nm, $C_r = 2.5$ Nm, $l_r = 1$ m;

mechanism for the vehicle to guide itself to a target location or to avoid obstacles. This decentralized control method is similar to Leonard and Fiorelli [9] and Rossetter [14] in that all of these methods use artificial potentials. While [14] uses virtual potentials to correct the vehicle to the referenced path and [9] uses artificial potentials to direct the group of vehicles in formation, this paper uses the virtual attractive and repulsive potentials to direct the vehicles towards way points while avoiding obstacles. In future work we propose to implement the model (4) on a collection of vehicles in which attractive-repulsive potentials between moving vehicles will allow them to self-organize into patterns. Preliminary results show anti-collision between two moving vehicles can be efficiently achieved by assigning the right repulsive and attractive potentials for their interaction. This anti-collision can be extended to not only two vehicles but to a group of vehicles. This work will likely involve a new generation of vehicles, the 'Bat' [8, 7], which has a hovercraft design capable of motion over rougher surfaces than the current MVWT lab floor. Porting the testbed to a larger area will allow the study of group formation in an arena that is not restricted by the large central post obstacle or near by side walls. Finally we note that the mapping from the motion laws in equation (4) to the Kelly equations (1-3) is straightforward and is portable to other platforms with second order dynamic vehicles.

ACKNOWLEDGMENTS

This research was supported by ONR grant N000140410054, ARO grant DAAD19-02-1-0055, NSF grants ACI-0321917 and DMS-9983726.

REFERENCES

[1] C.I. Connolly, J.B. Burns, R. Weiss. Path Planning Using Laplace's Equation, *in Proceeding IEEE Robotics and Automation Conference*, 1990.

[2] C.I. Connolly. Application of Harmonics Functions to Robotics, *in Proceeding of International Symposium on Intelligent Control*, 1992.

[3] B. Cook, D. Marthaler, C. Topaz, A. Bertozzi, and M. Kemp. Fractional Bandwidth Reacquisition Algorithms for VSW-MCM, *Multi-Robot System: From Swarm to Intelligent Automata*, vol. II, pages 77-86. Kluwer Academic Publishers, 2003.

[4] I.D. Couzin, J. Krause, R. James, G.D. Ruxton, and N.R. Franks. Collective memory and spatial sorting in animal groups, *J. Theor. Biol.*, vol. 218, pp. 1-11, 2002.

[5] L. Cremean, W. Dunbar, D.V. Gogh, J. Kickey, E. Klavins, J. Meltzer, R.M. Murray. "The Caltech Multi-Vehicle Wireless Testbed", *in Conference on Decision and Control*, 2002.

[6] W. Ebeling and U. Erdmann. Nonequilibrium statistical mechanics of swarms of driven particles, *Complexity*, vol. 8, no. 4, pp. 23-30, 2003.

[7] C. Hsieh, B.Q. Nguyen, D. Tung, L. Shi, Z. Jin, Y.L. Chuang, D. Marthaler, A. Bertozzi, R.M. Murray. "Joint UCLA-Caltech Report on the Implementation of Multi-agent Cooperative Control Algorithms", 2004. Available online: http://www.math.ucla.edu/∼bertozzi/MVWTproject/mvwt.html/.

[8] Z. Jin, S. Waydo, E.B. Wildanger, M. Lammers, H. Scholze, P. Foley, D. Held, and R.M. Murray, "MVWT-II: The Second Generation Caltech Multi-vehicle Wireless Testbed", *in 2004 American Control Conference*, Boston, MA, USA.

[9] N. E. Leonard, E. Fiorelli. "Virtual Leaders, Artificial Potentials and Coordinated Control of Groups", *in proceedings of 40th IEEE Decision and Control Conference*, 2001.

[10] H. Levine, W.J. Rappel, and I. Cohen. Self-organization in Systems of Self-propelled Particles, *Phy. Rev. E.*, vol.63, 017101, 2000.

[11] P. Ogren, N.E. Leonard. "Obstacle Avoidance in Formation", *in Proceedings of IEEE ICRA*, 2003.

[12] R. Olfati-Saber. Flocking for Multi-agent Dynamic Systems: Algorithms and Theory, *Technical Report CIT-CDS* 2004-005.

[13] J.K. Parrish and L. Edelstein-Keshet. Complexity, Pattern, and Evolutionary Trade-offs in Animal Aggregation, *Science*, vol. 294, pp. 99-101, 1999.

[14] E.J. Rossetter, J.P. Switkes, J.C. Gerdes. "A Gentle Nudge Towards Safety: Experimental Validation of the Potential Field Driver Assistance System", *in Proceeding of IEEE American Control Conference*, 2003.

[15] D. Tung, B.Q. Nguyen, C.H. Hsieh, Y.L. Chuang, Z. Jin, L. Shi, D. Marthaler, A.L. Bertozzi, R.M. Murray. "Experimental Implementation of an Algorithm for Cooperative Searching of Target Sites", september 2004, submitted *ACC 2005*.

[16] S. Waydo, R.M. Murray. "Vehicle Motion Planning Using Stream Functions", *in 2003 IEEE International Conference on Robotics & Automation*, Sept. 2003.